Cholinergic microvillous cells in the mouse main olfactory epithelium and effect of acetylcholine on olfactory sensory neurons and supporting cells

Tatsuya Ogura, Steven A. Szebenyi, [...], and Weihong Lin

Associated Data

Supplementary Materials

Abstract

The mammalian olfactory epithelium is made up of ciliated olfactory sensory neurons (OSNs), supporting cells, basal cells, and microvillous cells. Previously, we reported that a population of nonneuronal microvillous cells expresses transient receptor potential channel M5 (TRPM5). Using transgenic mice and immunocytochemical labeling, we identify that these cells are cholinergic, expressing the signature markers of choline acetyltransferase (ChAT) and the vesicular acetylcholine transporter. This result suggests that acetylcholine (ACh) can be synthesized and released locally to modulate activities of neighboring supporting cells and OSNs. In Ca^{2+} imaging experiments, ACh induced increases in intracellular Ca^{2+} levels in 78% of isolated supporting cells tested in a concentration-dependent manner. Atropine, a muscarinic ACh receptor (mAChR) antagonist suppressed the ACh responses. In contrast, ACh did not induce or potentiate Ca^{2+} increases in OSNs. Instead ACh suppressed the Ca^{2+} increases induced by the adenylyl cyclase activator forskolin in some OSNs. Supporting these results, we found differential expression of mAChR subtypes in supporting cells and OSNs using subtype-specific antibodies against M_1through M_5 mAChRs. Furthermore, we found that various chemicals, bacterial lysate, and cold saline induced Ca^{2+} increases in TRPM5/ChAT-expressing microvillous cells. Taken together, our data suggest that TRPM5/ChAT-expressing microvillous cells react to certain chemical or thermal stimuli and release ACh to modulate activities of neighboring supporting cells and OSNs via mAChRs. Our studies reveal an intrinsic and potentially potent mechanism linking external stimulation to cholinergic modulation of activities in the olfactory epithelium.

Keywords: transient receptor potential channel M5, muscarinic acetylcholine receptor, olfactory modulation, chemosensory, calcium imaging

ANIMALS RELY ON OLFACTION to find food and mates as well as to avoid predators and harmful environment. In mammals, the peripheral olfactory system consists of several anatomically segregated sensory apparatuses. Among these apparatuses, the main olfactory epithelium (MOE) houses the largest number of olfactory sensory neurons (OSNs) and plays a dominant role in detecting airborne odor molecules. The MOE, which lines the convoluted olfactory turbinates in the posterior nasal cavity, constitutes ~50% and 37% of the nasal surface area in rat and mice, respectively (Gross et al. 1982). Although this large surface area allows OSNs to interact maximally with odorants, the MOE is vulnerable to damage caused by xenobiotic agents including high levels of odor molecules, air pollutants, and microbial substances that may be present in inhaled air. In fact, the MOE is considered to be a major area for metabolizing xenobiotic substances (Ding and Dahl 2003). However, it is not known whether there are mechanisms allowing the activities of OSNs and supporting cells to be modulated on the basis of local interaction of xenobiotic substances to minimize potential chemical damage to the olfactory epithelium.

The trigeminal system is known to mediate sensory detection of inhaled irritants and harmful substances in the nasal respiratory epithelium, initiating protective reflexes. Trigeminal peptidergic nerve fibers expressing substance P and calcitonin gene-related peptide are abundant in the respiratory epithelium (Bryant and Silver 2000). Most of the intraepithelial trigeminal peptidergic nerve fibers are free nerve endings, which mediate sensory detection directly (Bryant and Silver 2000). Recently, studies on nasal solitary chemosensory cells (SCCs) have shown that some intraepithelial peptidergic nerve fibers actually innervate SCCs. These SCCs express chemosensory signaling components, such as transient receptor potential channel M5 (TRPM5), and respond to various chemical stimuli, including volatile irritants and bitter-tasting compounds, some of which are bacteria-secreted substances (Finger et al. 2003; Gulbransen et al. 2008; Lin et al. 2008b; Menini and Pifferi 2008; Ogura et al. 2010; Tizzano et al. 2010). This chemosensory cell-mediated detection of xenobiotic substances provides another mechanism for nasal chemical detection.

Although there is extensive trigeminal innervation in the nasal respiratory epithelium, intraepithelial trigeminal peptidergic nerve fibers are sparse in the MOE (Finger et al. 1990; Papka and Matulionis 1983). Also, the nasal SCCs are preferentially located at the anterior respiratory mucosa and are rarely found in the MOE (Finger et al. 2003; Lin et al. 2008a; Lin et al. 2008b). It is unlikely that SCCs mediate detection of xenobiotic substances in the MOE. Recently, Hegg et al. (2010) reported that some of the inositol 1,4,5-trisphosphate receptor type 3-expressing microvillous cells are innervated by trigeminal peptidergic nerve fibers and respond to a number of bioactive compounds and odor molecules. These results imply a potential important role of microvillous cells in chemical detection.

In the airway, there are other mechanisms that do not involve neuronal circuitry or reflexes, which interact with xenobiotic substances to facilitate the removal of such substances and minimize potential damage. It has been shown that ciliated epithelial cells and smooth muscle cells in the human airway express bitter-taste receptors and the phospholipase C signaling pathway. Together, they may detect bitter compounds secreted by microorganisms and facilitate their removal (Deshpande et al. 2010; Shah et al. 2009). In addition, some epithelial cells in the trachea can release acetylcholine (ACh) as a potent paracrine mediator to modulate both mucus secretion from secretory cells and ciliary movement of ciliated epithelial cells. This nonneuronal cholinergic regulation is important for airway clearance of foreign substances (Kummer et al. 2008; Stannard and O'Callaghan 2006). Presently, it is not known whether the tracheal epithelial cells that release ACh detect xenobiotic chemicals.

In the MOE, ACh has been shown to increase intracellular Ca^{2+} levels in supporting cells (Hegg et al. 2009). Also, ACh antagonists reportedly suppress odor-induced Ca^{2} increase (Firestein and Shepherd 1992; Li and Matsunami 2011). An early study using radioactive binding also indicates the presence of muscarinic ACh receptors (mAChRs), choline acetyltransferase (ChAT), and acetylcholinesterase (AChE) in salamander olfactory epithelium (Hedlund and Shepherd 1983). It is not known whether these cholinergic modulations present a mechanism to regulate olfactory activities according to local exposure of xenobiotic substances. Also, the source of ACh release and mechanisms that trigger the release are not determined.

The MOE is a pseudostratified structure that is comprised mostly of four distinct cell types: ciliated OSNs, supporting cells (called also sustentacular cells), basal cells, and microvillous cells (Farbman 2000). The OSNs make up the largest population of cells in the MOE and are responsible for detection of odor molecules. Their apical dendrites reach the luminal surface and form swelling dendritic knobs, from which multiple cilia emanate and interact with odor molecules in the mucus layer (Farbman 2000). Supporting cells are the second most abundant population of cells in the MOE. These cells span the entire thickness of the MOE with the nuclear regions of their cell bodies largely forming the superficial layer of the MOE (Vogalis et al. 2005a; 2005b). The apical portions of the supporting cells are covered with microvilli (Menco and Morrison 2003). Although the physiological functions of the supporting cells are not well understood, electrophysiological studies have shown that these cells are electrically coupled to each other (Vogalis et al. 2005a). In addition, these cells possess the large-conductance Ca^{2+}-activated K^+ currents (Trotier 1998) as well as voltage-gated Na^+ and K^+ currents capable of generating action potentials (Vogalis et al. 2005b). Furthermore, there is some evidence indicating that these cells play an important role in maintaining extracellular ionic gradients, secreting mucus, metabolizing noxious chemicals, and regulating cell turnover (Ding and Dahl 2003; Getchell and Mellert 1991; Menco and Morrison 2003).

Microvillous cells in the MOE are less abundant than supporting cells and OSNs. They are located primarily in the superficial layer of the olfactory epithelium, neighboring the supporting cells and OSNs, and are heterogeneous in morphology and potential functions. The most dominant feature of these cells is their apical microvilli, which reach the mucus layer and display various shapes and rigidness (Elsaesser and Paysan 2007; Hegg et al. 2010; Hansen and Finger 2008; Lin et al. 2008a; Menco and Morrison 2003). Recently, we and other investigators identified a population of TRPM5-expressing microvillous cells in the MOE using immunocytochemistry and transgenic mice, in which the expression of green fluorescent protein (GFP) is driven by the promoter of TRPM5 (Hansen and Finger 2008; Lin et al. 2008a). Because TRPM5 plays a critical role in chemical sensing in taste-receptor cells and SCCs (Finger et al. 2003; Ogura et al. 2010; Zhang et al. 2007), the TRPM5-expressing microvillus cells might also sense certain chemicals. However, unlike the SCCs, the TRPM5-

expressing microvillous cells are not innervated by trigeminal peptidergic nerve fibers (Hansen and Finger 2008; Lin et al. 2008a).

Recently, we discovered that the TRPM5-expressing SCCs of the vomeronasal organ (VNO) possess ChAT and vesicular acetylcholine transporter (VAChT), two key components for ACh synthesis and packaging in cholinergic cells (Ogura et al. 2010). This result extends our previous findings on the coexpression of TRPM5 and ChAT in the TRPM5-expressing taste-receptor cells of mice (Ogura et al. 2007). In taste buds, ACh modulates activities of the taste-receptor cells via both autocrine and paracrine mechanisms (Ogura 2002; Ogura and Lin 2005; Ogura et al. 2007). Because the microvillous cells we studied in the MOE also express TRPM5, we hypothesized that these cells are cholinergic and are capable of ACh synthesis and release.

In this study, we first sought to determine whether the TRPM5-expressing microvillous cells express ChAT and VAChT using transgenic mice and immunolabeling approaches. We then measured cholinergic modulation on isolated supporting cells and OSNs using an intracellular Ca^{2+} imaging method. In the intact MOE, these supporting cells and OSNs are neighbors with the microvillous cells. We also examined the expression of mAChR subtypes in the MOE. Furthermore, we sought to determine whether various xenobiotic chemical stimuli could activate the microvillous cells, possibly resulting in ACh release from these cells. Our results show that TRPM5-expressing microvillous cells are cholinergic and that ACh modulates activities of both supporting cells and OSNs via different subtypes of mAChRs. Our studies thus reveal a novel source of ACh release within the olfactory epithelium and a potential mechanism of linking nasal exposure of xenobiotic substances to cholinergic modulation of olfactory activities.

MATERIALS AND METHODS

Animals

Adult C57BL/6 background transgenic mice were used. The original mating pairs of TRPM5-GFP transgenic mice, in which the promoter of TRPM5 drives the expression of GFP, were kindly provided by Dr. Robert R.

Margolskee (Clapp et al. 2006) and were used in our previous studies for the identification of TRPM5-expressing cells in the nasal cavity (Lin et al. 2008a; 2007; 2008b; Ogura et al. 2010). The original ChAT$^{(BAC)}$-enhanced GFP (eGFP) transgenic mice were kindly provided by Dr. M. I. Kotlikoff (Tallini et al. 2006). In this mouse line, the expression of eGFP is driven by the endogenous ChAT transcriptional regulatory elements within a bacterial artificial chromosome (BAC). The expression of eGFP in cholinergic neuronal and nonneuronal cells has been characterized previously and shows excellent visualization of ChAT-expressing cells in both neuronal and nonneuronal tissues (Ogura et al. 2007; Tallini et al. 2006). Offspring were genotyped using the PCR for the presence of GFP. The original mAChR subtype M_3 knockout mice, which lack expression of M_3 subtype mAChR because of targeted gene disruption, were kindly provided by Dr. Jürgen Wess (Yamada et al. 2001). All animal care and procedures were approved by the Animal Care and Use Committees of University of Maryland, Baltimore County.

Immunocytochemistry

Tissue preparation.

Adult TRPM5-GFP, ChAT$^{(BAC)}$-eGFP, and ACh receptor M_3-knockout mice were deeply anesthetized with tribromoethanol (Avertin 250 μg/g body wt), perfused transcardially with 0.1 M phosphate buffer (PB) followed by a PB-buffered fixative containing 3% paraformaldehyde, 0.019 M L-lysine monohydrochloride, and 0.23% sodium M-periodate (Lin et al. 2007; 2008b). The nose was harvested, postfixed for 0.5–1 h, and transferred to 0.1 M PBS with 25% sucrose overnight. For immunolabeling of coronal MOE sections, the surrounding bones were removed before the tissues were embedded in optimal cutting temperature compound (Sakura Finetek USA, Torrance, CA). Unless otherwise mentioned, 14-μm-thick transverse sections were cut using a cryostat (Microm International, Walldorf, Germany), mounted onto Superfrost plus slides (Fisher Science, Pittsburgh, PA) and stored in a −80°C freezer until used.

Immunocytochemistry.

Sections of the MOE were thawed at room temperature, rinsed in 0.1 M PBS, and treated with 0.1 M NaOH for 1–5 min followed by three quick rinses of 0.1 M Na acetate and three 10-min washes with 0.1 M PBS. The sections were incubated in PBS-buffered blocking solution containing 2% normal donkey serum, 0.3% Triton X-100, and 1% bovine serum albumin for 1.5 h. For immunolabeling using subtype-specific antibodies against mAChRs, 0.5% Triton X-100 was used in blocking solution. For immunolabeling of VAChT, the tissue sections were rinsed and incubated in blocking solution with 0.5% Triton X-100 without antigen retrieval. Sections were then immunoreacted 48 to 72 h at 4°C with primary antibodies against each of the following proteins: PGP 9.5 (ubiquitin carboxyl-terminal hydrolase; 1:500, cat. no. AB1761; Chemicon, Temecula, CA), espin (1:300, cat. no. SC-133324; Santa Cruz Biotechnology, Santa Cruz, CA), ChAT (1:100, cat. no. AB144P; Millipore, Billerica, MA), VAChT (1:200, cat. no. V5387; Sigma, St Louis, MO), acetylated tubulin (1:20,000, cat. no. T7451, Sigma), M_1 mAChR (1:50 to 1:100, cat. no. AMR-001; Alamone Laboratories, Jerusalem, Israel), M_2 mAChR (1:250, cat. no. AMR-002, Alamone Labs; 1:250, cat. no. AB5166, Millipore), M_3 mAChR [1:500, cat. no. AS-3741S; Research & Diagnostic Antibodies (R&D), Benicia, CA; and 1:300, cat. no. M0194, Sigma], M_4 and M_5 mAChRs (1:500 and 1:250, cat. nos. AS-3761S and AS-3781S, R&D). For some experiments we also used anti-GFP (1:3,000, cat. no. ab13970; Abcam, Cambridge, MA) to intensify the GFP signal. After incubation of the primary antibodies, sections were then washed and reacted with donkey anti-rabbit secondary antibody (1:400, Alexa 555; Invitrogen, Eugene, OR), donkey anti-goat secondary antibody (1:400, Alexa 488, Invitrogen), donkey anti-mouse secondary antibody (1:400, Alexa 647, Invitrogen), and DyLight donkey anti-chicken secondary antibody (1:300; Jackson ImmunoResearch, West Grove, PA) for 1 h at room temperature. Sections were mounted on slides with Fluoromount-G (SouthernBiotech, Birmingham, AL). In controls for these experiments, primary antibodies were removed, resulting in negative labeling.

Image acquisition.

For direct visualization of GFP expression and counting of GFP-positive cells, the nose was split along the midline to expose the nasal cavity. Low

magnification pictures were taken using an Olympus BX 41 compound microscope equipped with epifluorescence. High-magnification images of immunolabeled sections were taken using an Olympus BX 61 epifluorescence microscope equipped with a spinning disc confocal unit.

Cell counting.

After the ChAT$^{(BAC)}$-eGFP mice were fixed, the nose was split along the midline. The olfactory epithelia lining the dorsal recess and septum were stripped, spread out, mounted onto microscope slides with fluoromount-G, and imaged at low magnification (×4) using an Olympus epifluorescence microscope. For epithelium lining the olfactory turbinates, multiple ×4 images with varied focus planes were taken at random regions and composited. ChAT(GFP)-expressing cells were counted, and surface areas were measured using an NIH ImageJ program. Manual counting was also conducted in some specimens to ensure accurate estimation.

Intracellular Ca^{2+} Imaging on Isolated Cells of the MOE

Solutions and chemicals.

The bath solution (Tyrode's saline) contained (in mM): 140 NaCl, 5 KCl, 10 *N*-2-hydroxyethylpiperazine-*N*′-2-ethanesulfonic acid buffer (HEPES), 1 $MgCl_2$, 3 $CaCl_2$, 10 Na pyruvate, and 10 D-glucose (pH 7.4). ACh, atropine, ATP, and denatonium benzoate were made up in stock solution and diluted with Tyrode's into various concentrations. All these chemicals were purchased from Sigma. Forskolin (Calbiochem, San Diego, CA) was dissolved in DMSO in stock of 10 mM and diluted into the bath solution to a final concentration of 1 μM. Odorous chemicals were obtained from Sigma-Aldrich at the highest purity available. Odorants were made by dilution with vigorous vortexing, and stocks of odorants were stored at −20°C.

Procedure for Mycobacterium smegmatis lysate preparation.

Mycobacterium smegmatis (*M. smegmatis*) colonies were picked and cultured in 200 ml of Luria broth in a 37°C incubator with vigorous shaking for a period of 48 h. The culture was then centrifuged at 4,500 revolution/min for

10 min at 4°C. Pellets obtained from 15 ml of culture were resuspended in 5 ml of Tyrode's solution. The resuspended solution was then French pressed at 1,200 psi, and the lysate obtained was dialyzed in Tyrode's solution using size no. 8 dialyzer tubing (VWR, Radnor, PA) overnight. The resulting dialyzed solution was used in physiology experiments.

Enzymatic isolation of cells in the MOE.

The method of cell isolation was adapted from our previous study (Lin et al. 2008b; Ogura et al. 2010). Briefly, TRPM5-GFP or ChAT$^{(BAC)}$-eGFP mice were euthanized by CO_2 exposure. The head skin was removed before the nose was split down the midline. The olfactory tissues were dissected, cut into small pieces, and placed in Ca^{2+}-Mg^{2+}-free Tyrode's saline with about 4 U/ml of papain (Worthington, Lakewood, NJ) and 2 mM cysteine for 3–5 min with brief vortexing or 15–30 min without vortexing at room temperature. Gentle pipetting at the end of enzyme incubation was applied to facilitate the cell dissociation. The supernatant was transferred to an O-ring chamber on a cover slip precoated with concanavalin A (Sigma).

Fura-2 ratio Ca^{2+} imaging.

After the freshly isolated cells were settled, the bath solution was replaced with Tyrode's saline containing 2 μM fura-2 AM (Invitrogen) for 20 min and washed with normal Tyrode's. Excitation wavelength was alternated between 340 and 380 nm using a filter wheel incorporated with a xenon lamp system (Lambda LS; Sutter Instruments, Novato, CA). The excitation light was guided via a liquid optical fiber to an inverted microscope (Olympus IX71). The ratio of fluorescence intensity at excitation wavelengths of 340 and 380 nm indicated the intracellular Ca^{2+} levels. Fluorescent images were obtained with a ×40 oil UV objective lens (N.A. 1.3) with a 510 ± 42 nm emission filter (Semrock, Rochester, NY). Imaging Workbench software version 5.2 (INDEC BioSystems, Santa Clara, CA) was used to capture images and to change the position of the filters. Pairs of images at the two wavelengths were usually acquired every 3 s. In experiments where we determined the effects of the extracellular Ca^{2+} on ACh-induced Ca^{2+}responses, the bath solution was replaced with nominal extracellular $CaCl_2$ solution in which the $CaCl_2$ was omitted from the Tyrode's saline. We considered a change in the intracellular Ca^{2+} levels (ratio of F340/F380) to be a stimulus-induced

response if the peak value of the change during stimulation was greater than two standard deviations above the mean resting level, which was obtained by averaging 10 data points (3 s each) before applying the stimulus in each cell tested (Ogura et al. 2010; 1997).

Statistical Analyses

For comparison of Ca^{2+} imaging data of supporting cells, a one-tailed Student's *t*-test was performed. $P < 0.05$ was considered to be statistically different. To separate ACh-sensitive OSNs and ACh-nonsensitive OSNs from pooled Ca^{2+} imaging data, cluster analysis using Ward's method was applied. To evaluate the quality of clustering, we computed the cophenetic correlation coefficient for effective comparison between dendrograms (Sokal and Rohlf 1962). Bar graphs represent the mean percent change at the peak response from resting Ca^{2+} levels ± SE.

RESULTS

ChAT-Expressing Microvillous Cells in MOE

We determined whether ACh can be synthesized and released intrinsically by microvillous cells of the MOE by monitoring the expression of ChAT, a key enzyme for ACh synthesis using transgenic $ChAT^{(BAC)}$-eGFP mice. In a whole-mount preparation of olfactory epithelium (OE), we found bright GFP fluorescence exclusively in microvillous cells throughout the entire MOE as well as the septal organ (Fig. 1, *A* and *B*). On average, there are about 1,197 ± 40 GFP-expressing cells/mm^2 surface area ($n = 7$ mice). This cell density of ChAT-expressing microvillous cells is very close to the cell density of TRPM5-expressing microvillous cells (1,158 cells/mm^2 surface area reported in our previous study; Lin et al. 2008a). The GFP-expressing microvillous cells are confined in the OE and are absent from the immediate adjacent respiratory epithelium, a spatial distribution pattern identical to the TRPM5-expressing microvillous cells we reported previously (Lin et al. 2008a). In coronal sections, the GFP-expressing cells are superficially located with their apical microvilli reaching to the epithelial surface (Fig. 1*C*). Similar to the TRPM5-expressing microvillous cells, the GFP-expressing cells from the $ChAT^{(BAC)}$-eGFP mice also did not immunoreact to an antibody against the

neuronal marker PGP 9.5, which labels OSNs (Fig. 1*C*). Thus the GFP-positive cells are not neurons. Furthermore, the GFP-expressing cells resemble the TRPM5-expressing microvillous cells in morphology, showing various shapes of cell body and apical microvilli (Lin et al. 2008a), which can be appreciated in the figures throughout this paper. To better visualize the apical microvilli, we used an anti-GFP antibody to intensify the GFP signal. Two representative images of GFP-immunolabeled microvillous cells from ChAT$^{(BAC)}$-eGFP and TRPM5-GFP mice are shown in Fig. 1, *D* and *E*, respectively. The apical processes of GFP-expressing microvillous cells from both ChAT$^{(BAC)}$-eGFP and TRPM5-GFP mice were labeled with an antibody against espin (Fig. 1, *F* and *G*), an actin cytoskeletal bundling protein found in microvilli of many sensory cells (Sekerkova et al. 2004). Additionally, there is no axon emanating from the basal region of the GFP-expressing microvillous cells. Some GFP-expressing microvillous cells show a single short basal process, which usually does not reach the basal lamina, except in the area where the MOE is thin or near the junction with the respiratory epithelium. Thus the GFP-expressing microvillous cells we observed in the ChAT$^{(BAC)}$-eGFP show identical properties with the TRPM5-expressing microvillous cells in the olfactory epithelium (Hansen and Finger 2008; Lin et al. 2008a).

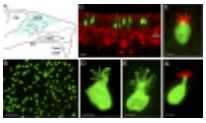

Fig. 1.

Identical properties shared by choline acetyltransferase green fluorescent protein (ChAT GFP)-expressing and transient receptor potential channel M5 (TRPM5)-expressing microvillous cells. *A*: schematic drawing of a mouse hemi-nose, showing distribution ...

TRPM5-Expressing Microvillous Cells Immunoreact to Antibodies Against ChAT and VAChT

To confirm that ChAT is indeed present in TRPM5-expressing microvillous cells, we immunolabeled MOE sections of ChAT$^{(BAC)}$-eGFP and TRPM5-GFP mice with an antibody against ChAT. As shown in Fig. 2, *A*–*C*, ChAT immunoreactivity was found in all the GFP-expressing microvillous cells in the MOE sections of both lines of transgenic mice. Also, we determined the

expression of VAChT, a transporter protein required for packaging ACh into vesicles. We found positive immunoreactivity for VAChT in the GFP-expressing microvillous cells of both ChAT$^{(BAC)}$-eGFP and TRPM5-GFP mice (Fig. 2, *D–F*). The immunoreactivity for both ChAT and VAChT is strong in the cell body (Fig. 2, *G*and *H*). Positive labeling for these two antibodies was also observed in nerve fibers innervating submucosal glands, as well as neuromuscular junctions known to express both ChAT and VAChT (data not shown). These results clearly demonstrate that TRPM5-expressing microvillous cells are cholinergic. Thus ACh can be synthesized and released locally by the TRPM5/ChAT-expressing cells within the MOE.

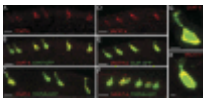

Fig. 2.

Immunoreactivity of ChAT and vesicular acetylcholine transporter (VAChT) in the GFP-expressing microvillous cells. *A*: confocal image showing positive ChAT immunoreactivity (ChAT-ir; red) in the microvillous cells of a ChAT$^{(BAC)}$-eGFP mouse. *B*: image of ...

Intracellular Ca^{2+} Responses to ACh in TRPM5/ChAT-Expressing Microvillous Cells

ACh in the nervous system and nonneuronal tissues can act either via autocrine mechanisms to modulate the activities of the releasing cells or via paracrine mechanisms to influence the activities of neighboring cells (Resende and Adhikari 2009; Wessler and Kirkpatrick 2008). We examined whether ACh induces responses in TRPM5/ChAT-expressing microvillous cells, neighboring supporting cells, and OSNs. We freshly isolated cells from the MOE of either ChAT$^{(BAC)}$-eGFP or TRPM5-GFP mice, loaded them with a Ca^{2+}-sensitive dye fura-2 AM, and monitored the changes in intracellular Ca^{2+} levels in Ca^{2+} imaging experiments. Isolated TRPM5/ChAT-expressing microvillous cells were identified by their strong GFP expression and morphological features, such as apical microvilli, relatively smaller size, and the absence of dendritic knobs that are present in OSNs (Lin et al. 2008a). We stimulated these cells with 100 μM ACh because the EC_{50} for ACh to induce Ca^{2+} changes in sensory cells is reported in the range of 10^{-6} to 10^{-5} M (Dasso et al. 1997; Ogura 2002; Rome et al. 1999). Only one of the 45

ChAT/TRPM5 microvillous cells tested from 14 mice responded to ACh (100 μM), and the response amplitude was very small (<5% changes from the resting level; data not shown), compared with the ACh responses in supporting cells detailed in the following paragraph. Thus it is very unlikely the ACh released from these cells would function to regulate their own activity via an autocrine mechanism.

Intracellular Ca^{2+} Responses to ACh in Supporting Cells

We next investigated whether ACh modulates activity of neighboring cells via paracrine mechanisms. Supporting cells in the MOE are neighbors with microvillous cells. These cells are known to have glia-like properties and may support OSNs physically and physiologically as well as metabolize xenobiotic substances (Carr et al. 2001; Ding and Dahl 2003; Getchell and Mellert 1991; Menco and Morrison 2003; Trotier 1998; Vogalis et al. 2005a; 2005b). We used the following criteria to identify supporting cells in isolated cell populations: lack of GFP expression, absence of dendritic knobs, and presence of short and relatively uniformed apical microvilli emanating from a region close to the cell body. The putative supporting cells generally have a long and stout basal process when freshly isolated (Fig. 3*A*, *inset*, and Supplemental Video S1; supplemental material for this article is available online at the *Journal of Neurophysiology* website). As time went on, these cells tended to round up and their basal processes shortened to various lengths. Bath application of ACh (100 μM) induced increases in Ca^{2+} levels in 78% of supporting cells tested (73 cells responded out of 93 cells, 27 mice). The ACh-induced response was repeatable in a single cell for several times in isolated condition. Furthermore, we conducted some experiments using small pieces of olfactory turbinate and monitored ACh-induced responses in the superficial layer containing mostly supporting cells (n = 3 pieces of turbinates from 3 mice). The layer of supporting cell bodies was determined using the location of GFP-positive microvillous cells, which reside in the superficial layer and neighbor with cell bodies of supporting cells (Fig. 3*B*, *inset*). We found that ACh induced Ca^{2+}increases in many presumed supporting cell bodies in the superficial layer, and the responses are comparable to the responses obtained from the isolated supporting cells (Fig. 3*B*). Thus ACh is a potent activator for supporting cells.

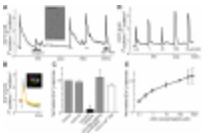

Fig. 3.

ACh-induced increases in intracellular Ca^{2+} levels in supporting cells. *A*: representative recording from a single supporting cell showing Ca^{2+} responses to 5 applications of ACh (100 μM), as indicated by the black horizontal bars. The second response ...

We next examined whether ACh-induced responses are mediated by the mAChRs. We used atropine (0.5 μM), an antagonist common to all five mAChR subtypes, to antagonize the effect of ACh. We chose a dose of 0.5 μM on the basis of published studies that show the antagonist affinity constants of atropine on mammalian mAChR are around 10^{-9} M and the values are similar for all five subtypes (Caulfield and Birdsall 1998; Dasso et al. 1997; Hegg et al. 2009; Ogura 2002; Shigemoto and Ohmori 1990). As shown in Fig. 3*A*, the ACh-induced responses were greatly reduced in the presence of atropine (0.5 μM), an antagonist of mAChRs. The effect of atropine was reversible, and the ACh-induced Ca^{2+}increases could be fully recovered (n = 4 cells, 4 mice). In the control group (n = 4 cells, 3 mice), we repeatedly stimulated each individual supporting cell with 100 μM ACh in the same condition. Figure 3*C* presents normalized and averaged Ca^{2+} response amplitudes from both control and experimental groups. We measured the induced percent changes of Ca^{2+} values from the resting levels and normalized the second response value to the value of the first response in each individual cell. The averaged first and second response amplitudes are similar in the control group, whereas suppression by atropine is statistically significant (paired t-test, $P < 0.05$). This result demonstrates that the ACh induced Ca^{2+}increases in the supporting cells largely via mAChRs. In addition, we determined the source of Ca^{2+} increases induced by ACh. The ACh-induced Ca^{2+} increases generally showed two phases. The initial phase is transient and decays rapidly, which is followed by a slow decay phase (see Fig. 3*A*). The slow decay phase was more evident when ACh was applied for a relatively long period of time (data not shown). In Ca^{2+}-free saline, we found that the initial transient component persisted, whereas the slow decay phase largely disappeared (Fig. 3*A*, Ca^{2+} free). As shown in Fig. 3*C*, the normalized peak responses of the transient component in the Ca^{2+}-free saline was 0.86 ± 0.05 (n = 12 cells, 12 mice), which is comparable to the

normalized value of second responses in normal saline. Thus the initial ACh-induced Ca^{2+} increases are due to Ca^{2+} release from internal Ca^{2+} stores. Furthermore, we determined whether the Ca^{2+} increases depend on the concentrations of ACh. Individual isolated supporting cells were challenged by various concentrations of ACh from 0.1 μM to 1 mM in random order (Fig. 3*D*). The amplitudes of ACh responses were concentration dependent. The normalized response curve is presented in Fig. 3*E*, showing that the supporting cells are very sensitive to ACh. Together these data demonstrate that the intracellular Ca^{2+} levels in supporting cells can be strongly influenced by ACh via muscarinic receptor-mediated paracrine mechanisms.

Intracellular Ca^{2+} Responses to ACh in OSNs

We next examined the effect of ACh on isolated OSNs in Ca^{2+} imaging. Individual OSNs were identified primarily on the basis of the presence of morphological features, including an apical dendrite, dendritic knob, and long cilia emanating from the dendritic knob (Fig. 4*A* and Supplemental Video S2). In TRPM5-GFP mice, because TRPM5 is also expressed in a subset of OSNs (Lin et al. 2007), some OSNs were GFP positive. However, these OSNs generally exhibited much weaker GFP than the TRPM5-expressing microvillous cells (Lin et al. 2008a; 2007). We recorded both GFP-positive and negative OSNs. Because there was no apparent difference in the effects of ACh between the GFP-positive and -negative OSNs, in the following experiments, we pooled the results. We first tested responses of isolated OSNs to an odor mixture containing 1-pentanol, phenethyl alcohol, pentyl acetate, geraniol, and citral (each 10 μM). About 20% of OSNs tested responded with sharp increases in intracellular Ca^{2+} levels in both the dendritic knobs and somata of the OSNs (Fig. 4*B*; 31 out of 157 cells, 13 mice tested). Unlike in supporting cells, ACh (100 μM) failed to induce measurable increases in intracellular Ca^{2+} levels in OSNs (Fig. 4*B* $n = 62$ cells, 23 mice). To ensure the tested cells were physiologically functional, we tested responses to forskolin, which directly activates adenylyl cyclase type III (ACIII), mimicking odor-induced responses via the canonical cAMP signaling pathway (Fig. 4*B*) (Lin et al. 2004). Nearly all OSNs tested responded to forskolin (1 μM) with increases in Ca^{2+} levels. Interestingly, some OSNs displayed spontaneous Ca^{2+} oscillations. ACh applied to the bath solution suppressed the amplitude of Ca^{2+} oscillations in 18 out of 23 cells

from 19 mice tested (Fig. 4*C*). The Ca^{2+} oscillations depended on extracellular Ca^{2+}, as replacing the bath solution with Ca^{2+} free saline diminished the oscillations. These results indicate that ACh may exert its effect when OSNs are activated.

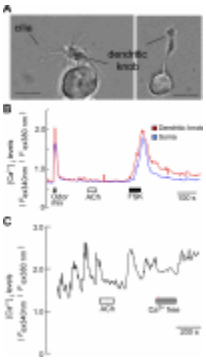

Fig. 4.

ACh fails to increase Ca^{2+} levels but suppresses spontaneous oscillation in some OSNs. *A*: images of 2 isolated OSNs. Long cilia are preserved intact after the isolation process. Scale bar = 5 μm. *B*: isolated OSN responded to an odor mixture (10 ...

To further investigate the possible inhibitory effect of ACh on the activated OSNs, we stimulated OSNs with forskolin (1 μM). As shown in Fig. 5*A*, forskolin induced large Ca^{2+}increases in both dendritic knobs and cell bodies (Fig. 5*A*, *left*). Because there were various degrees of variation in the repeated response amplitudes in a single cell, we applied forskolin three times to each individual OSN in the control group (Fig. 5*A*, *left*) and normalized the second and third responses to the first responses. The normalized Ca^{2+}responses to repeat forskolin stimulation measured from the dendritic knobs and somata of individual OSNs are plotted (Fig. 5*B*, labeled as "FSK", n = 6 cell, 3 mice). In the experimental groups, we applied the same concentration of forskolin three times with the second application either in the presence of ACh alone (100 μM, n = 15 cells, 7 mice, Fig. 5*A*, *middle*) or ACh plus atropine at 0.5 μM (n = 14 cells, 6 mice, Fig. 5*A*, *right*) or at 5 μM (n = 12 cells, 5 mice). Similar to control experiments, the normalized Ca^{2+}responses in the presence of ACh or atropine plus ACh were plotted (Fig. 5*B*, labeled as "ACh +FSK" and "Atropine + ACh + FSK"). We found that the OSNs tested could be clustered into ACh-suppressed and ACh-insensitive groups using the cluster analysis of Ward's method (Ward 1963). To evaluate the quality of clustering, we computed the cophenetic correlation coefficient for effective comparison

between clusters (Sokal and Rohlf 1962). The coefficients are 0.869 and 0.829 for dendritic knobs and somata, respectively. The OSNs in the ACh-suppressed group show reduction of forskolin-induced Ca^{2+} increases in the presence of ACh. The suppression was recoverable after washing away ACh with normal saline (Fig. 5*A*, *middle*). Statistical data analyses show the data from the ACh-suppressed group (n = 7 cells from 7 mice and 6 cells from 4 mice for dendritic knobs and somata, respectively) are significantly different from data from the ACh-insensitive group (Fig. 5, *B* and *C*, n = 8 cells from 6 mice and 9 cells from 5 mice for dendritic knobs and somata, respectively, ** t-test, $P < 0.01$). Furthermore, the data of the ACh-suppressed group are significantly different from data of the control experiment without ACh (t-test assuming unequal variances, $P < 0.01$). In the presence of atropine, the effects of ACh no longer can be clustered. Moreover, the averaged response amplitudes in both somata and dendritic knobs in the presence of atropine are significantly different from the data of the ACh-suppressed group (Fig. 5, *B* and *C*, Atropine+ACh, t-test, $P < 0.01$), whereas there is no significant difference from the control response amplitudes (Fig. 5*C*). An increase in the concentration of atropine to 5 μM did not alter the results (n = 14 cells from 5 mice, Fig. 5, *B* and *C*, Atropine+ACh, t-test, $P < 0.01$). We also tested ACh effects on odor mixture-induced Ca^{2+} responses in some OSNs. Similarly, ACh did not potentiate odor mixture-induced Ca^{2+} increases. Instead, ACh suppresses the Ca^{2+} increases in some cells (data not shown). These results strongly suggest that ACh suppresses evoked activity in some OSNs via mAChRs, most likely the inhibitory subtypes, such as M_2 and M_4.

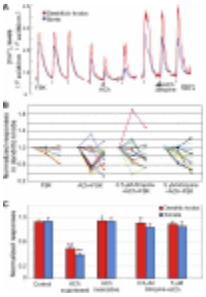

Fig. 5.

ACh-mediated suppression of forskolin-induced Ca^{2+} increases in some OSNs. *A*: 3 representative recordings of Ca^{2+} responses to forskolin (1 μM). *Left*: forskolin was applied 3 times as indicated by vertical bars. *Middle*: 2nd response to forskolin ...

Expression of Subtypes of mAChR in the MOE

Our results from Ca^{2+}-imaging experiments revealed two pieces of important information. First, ACh differentially affects supporting cells and OSNs, suggesting that these cells express different ACh receptors. Second, the effects of ACh in both the supporting cells and OSNs are suppressed by atropine, indicating the involvement of the mAChRs. We focused on the expression of mAChR subtypes. It is well known that activation of M_1 and M_3 produces stimulating effects, such as an increase in intracellular Ca^{2+} levels, whereas activation of M_2 and M_4 leads to negative regulation of adenylyl cyclases and suppression of cell activities (Caulfield and Birdsall 1998; Felder 1995). The effect of M_5 is less understood. Using subtype-specific antibodies in immunolabeling, we examined the expression of mAChR subtypes in MOE sections of either TRPM5-GFP or $ChAT^{(BAC)}$-eGFP mice. Because TRPM5 is expressed in the microvillous cells and a subset of mature OSNs (Lin et al. 2008a; 2007), the GFP expression marks both cell types. Figure 6 shows the immunoreactivity for stimulatory subtype M_1 AChR. The antibody against the M_1 subtype reacted strongly to the olfactory epithelium in the lateral and ventral regions, whereas there is no apparent labeling in the dorsal and medial regions of the MOE (Fig. 6, *A–D*). In areas where there was strong M_1 immunoreaction, we found positive reaction in supporting cells (Fig. 6*C*). Although there was strong immunoreaction in the region where cells bodies of OSNs are located, the label apparently did not colocalize with OSNs. Instead, it seemed to embrace the OSNs (Fig. 6*D*). Because supporting cells extend the entire thickness of the epithelium (see Fig. 3, *inset* for an isolated supporting cell), the antibody against M_1 may label basal regions of supporting cells.

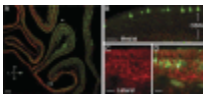

Fig. 6.

Immunoreactivity of muscarinic AChR subtype M_1 in the MOE. *A*: low-magnification confocal image from a coronal section of the MOE from a TRPM5-GFP mouse. The M_1immunoreactivity (red) is primarily present in lateral region. *B*: confocal image from a dorsal-medial ...

We used two antibodies to label the M_3 subtype. The antibody purchased from R&D labeled the supporting cells, particularly in their cell bodies located in the superficial layer (Fig. 7*A*). The basal processes of supporting cells were also labeled. To verify the specificity of this antibody, we obtained MOE sections from the mAChR subtype M_3 knockout mice and immunoreacted these sections along with the sections from ChAT$^{(BAC)}$-eGFP mice under the same conditions (Fig. 7, *A* and *B*). The M_3 knockout abolished the M_3immunoreaction in the MOE (Fig. 7*B*). To determine whether there is M_3 expression in the cilia, we double-labeled MOE sections using the R&D anti-M_3 AChR antibody and another antibody against acetylated tubulin, which labels OSN cilia. As shown in Fig. 7*C*, the R&D anti-M_3 AChR antibody labeled the supporting cells, but not the cilia. Upon further examination of the immunoreactivity in sections from the TRPM5-GFP mice, in which the TRPM5-expressing OSNs are GFP positive (Lin et al. 2007), we found that the immunoreactivity to M_3 in the OSN cell body layer is very weak or absent (Fig. 7*D*), suggesting that there is little or no M_3 expression in cell bodies of OSNs (see also Fig. 7*C*OSN cell body region). The other anti-M_3 AChR antibody we used was purchased from Sigma (Fig. 7, *E* and *F*). In most regions of the MOE sections, we found that the Sigma anti-M_3 antibody strongly labeled the supporting cells only (Fig. 7E) and that M3 knockout completely abolished this labeling in supporting cells (Fig. 7*F*). This result is the same as that obtained using the R&D antibody. However, in some ventral regions of the MOE, the Sigma antibody labeled supporting cells, OSNs, and axon bundles. The reactivity in these OSNs was especially obvious in the dendritic knobs. However, the reaction in these OSNs was not abolished in sections of the M_3 AChR knockout. Thus it appears that the labeling in these OSNs by the Sigma antibody is nonspecific to the M_3 AChR (data not shown). These results strongly suggest that the supporting cells express stimulating subtypes, especially the M_3 mAChR.

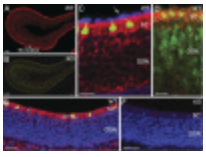

Fig. 7.

Strong immunoreactivity of muscarinic AChR subtype M_3 in supporting cells of the MOE. *A–D*: immunolabeling results using the Research & Diagnostic (R&D) anti-M_3 antibody. *E*and *F*: immunolabeling results using the Sigma anti-M_3 antibody. ...

We next examined the expression of inhibitory subtypes, M_2 and M_4 of mAChRs in OSNs. We found that the antibody against the M_2 did not label OSNs and supporting cells in most regions of the MOE. Only in some ventral regions of the MOE, supporting cells seemed to be labeled (data not shown). The immunoreactivity for M_4 subtype is largely limited to OSNs. Both apical cilia and cell bodies were labeled (Fig. 8, *A* and *B*). The anti-M_5 antibody also labeled the OSNs with most of the activity found in the cell bodies (Fig. 8, *C* and *D*). Interestingly, none of the subtype-specific antibodies labeled the TRPM5/ChAT-expressing microvillous cells. These immunolabeling results demonstrate that OSNs and supporting cells differentially express mAChR subtypes. The expression of stimulatory M_3 in supporting cells and inhibitory M_4 in OSNs strongly supports our data obtained in Ca^{2+} imaging.

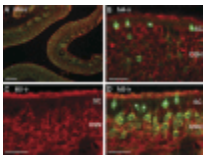

Fig. 8.

Immunoreactivity of muscarinic AChR subtypes M_4 and M_5 in OSNs of TRPM5-GFP mice. *A* and *B*: low- and high-magnification confocal images of the M_4 immunoreactivity (red) in OSNs. *C*: image of M_5 immunoreactivity (red) in cell bodies of OSNs. *D*: GFP image ...

Chemical Stimuli-Induced Ca^{2+} Responses in TRPM5/ChAT-Expressing Microvillous Cells of the MOE

The data we have described strongly indicate that the TRPM5/ChAT-expressing microvillous cells of the MOE are capable of releasing ACh, which modulates the activities of neighboring supporting cells and OSNs via mAChRs. However, what may trigger these microvillous cells to release ACh is not known. Because these cells express TRPM5, an ion channel known to be involved in chemical sensing in a various chemosensory cells including SCCs in the nasal cavity (Gulbransen et al. 2008; Lin et al. 2008b; Ogura et

al. 2010; Tizzano et al. 2010), and because the MOE is constantly exposed to inhaled chemicals, we reasoned that these microvillous cells may be chemosensitive. In particular, they may function to detect harmful substances and agents because their apical microvilli are in the mucus layer. We freshly isolated GFP-positive microvillous cells from the ChAT$^{(BAC)}$-eGFP mice and monitored intracellular Ca^{2+} levels in these cells. Figure 9*A*, *inset* shows a GFP-positive microvillous cell in isolated condition. We tested various chemicals, including ATP, which can be released when cells or bacteria are broken, high levels (0.5 mM) of volatile odorants, such as citral (plant product) and lilial, and soil bacteria lysate (*M. smegmatis*). As stated previously, application of ACh generally did not induce Ca^{2+} increases (Fig. 9*A*). About 38% of the cells responded to 100 μM ATP (5 out of 13 cells tested from 9 mice). More than 50% of the cells also responded to citral and lilial with increases in Ca^{2+} levels (Fig. 9*B*; 4 out of 7 cells from 4 mice, and 5 out of 7 cells from 4 mice tested, respectively). Some individual cells responded to multiple stimuli. Often these cells showed spontaneous Ca^{2+} oscillation at resting condition, and, as shown in Fig. 9*C*, the responses to bacterial lysate and ATP were oscillatory and added onto the spontaneous oscillation, showing overall enhancement of the amplitude (Fig. 9*C*). Approximately 19% of the cells tested responded to the application of soil bacterium lysate (10 of 53 cells, 9 mice). Furthermore, we examined whether a bitter-tasting compound would induce Ca^{2+} responses in the microvillus cells because bacterial and fungal products often taste bitter to animals (Brockhoff et al. 2007). Approximately 33% of the tested TRPM5/ChAT-expressing microvillus cells from four mice responded to denatonium benzoate (3 mM). These results indicate that the TRPM5/ChAT-expressing microvillus cells are sensitive to a variety of chemical stimuli. In addition to the chemosensitivity, the microvillous cells are also sensitive to changes in bath temperature. Most of the microvillus cells tested showed increases in Ca^{2+} levels in response to a temperature drop in the bath solution from 20 to 4°C (Fig. 9*D*; 23 out of 28 cells, 5 mice). Because temperature of inhaled air varies and cold air is potentially harmful to the lower airway, this thermosensitivity may play a role in triggering mechanisms to warm the inhaled air before reaching the lower airway and the lung. These results are summarized in Fig. 8*E*. Taken together, our data suggest that TRPM5/ChAT-expressing microvillus cells can be activated by external chemo- or thermostimulation.

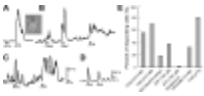

Fig. 9.

Chemo- and thermostimuli induced Ca^{2+} increases in a subset of ChAT-expressing microvillous cells. *A* and *B*: representative traces from two isolated ChAT-expressing microvillous cells. Application of ACh (100 μM) did not induce changes in intracellular ...

DISCUSSION

The exquisite sensitivity of the olfactory epithelium relies on the proper functioning of the OSNs along with a well maintained and consistent local extracellular environment. Being a significant part of the nasal mucosa, the OE is exposed to a wide variety of inhaled chemicals including irritating and harmful xenobiotic substances. Thus regulating activities of supporting cells and OSNs according to local chemical exposure may be critical for maintaining olfactory sensitivity and integrity, as well as protecting the epithelium from chemical-induced damage. In this study, we show that the signature cholinergic proteins ChAT and VAChT are present in TRPM5-expressing microvillous cells and that these cells are sensitive to chemical and thermal stimulation. We also show that ACh modulates activities of supporting cells and OSNs differently, which strongly correlates with the expression of mAChR subtypes in these cells. Our studies, therefore, provide a novel insight into the physiological function of TRPM5/ChAT-expressing microvillous cells and demonstrate a source of intrinsic ACh release in the MOE, thereby linking local chemical exposure to the cholinergic modulation of olfactory activities.

Cholinergic Properties of TRPM5-Expressing Chemosensory Cells

Previously, we reported that both TRPM5-expressing taste-receptor cells and SCCs of the VNO in mice express ChAT and VAChT (Ogura et al. 2010; 2007). Our present results further reveal another population of TRPM5-expressing cells that are cholinergic. Together, these results reveal a common ability of synthesizing and releasing ACh in TRPM5-expressing nonneuronal chemosensory cells. Interestingly, TRPM5-expressing

chemosensory cells are present in other parts of the airway (Kaske et al. 2007; Tizzano et al. 2011; our unpublished observations) and the gastrointestinal tract (Bezencon et al. 2008), where ChAT-expressing epithelial cells have also been reported (Kummer et al. 2008; Tallini et al. 2006). The similarity of morphological appearances suggests that they are the same cell type coexpressing TRPM5 and ChAT (Kummer et al. 2008). In taste-receptor cells of the taste bud, ACh activates the phospholipase C signaling pathway via mAChR subtype M_1 (Ogura 2002). The same pathway also mediates taste transduction of sweet, bitter, and umami substances. Potentially, ACh can exert strong modulation on the taste signal transduction. In the VNO, SCCs are heavily innervated by trigeminal peptidergic nerve fibers (Ogura et al. 2010). It remains to be determined whether these SCCs release ACh as a neurotransmitter to relay sensory information onto the trigeminal nerve fibers or as autocrine or paracrine mediators. Unlike SCCs, the TRPM5/ChAT-expressing microvillous cells in the MOE are not innervated by trigeminal peptidergic nerves. ACh released from these microvillous cells upon activation by external stimuli likely functions as a paracrine mediator to modulate activities of neighboring supporting cells and OSNs. ACh-mediated autocrine regulation on the microvillous cells appeared minimal, as we found that these cells usually do not respond to ACh nor express mAChRs. Our present studies do not rule out the expression of nicotinic AChRs in these cells.

ACh-Mediated Regulation of Supporting Cells

In our Ca^{2+}-imaging experiments, supporting cells of the MOE showed robust responses to ACh with an increase in intracellular Ca^{2+} levels. This result is supported by the positive immunolabeling of stimulating subtypes of mAChR especially M_3 in these cells. Activation of the stimulatory mAChRs is known to induce increases in intracellular Ca^{2+}levels (Caulfield and Birdsall 1998; Ogura et al. 2002). Our results are also in agreement with the previous report in which atropine suppresses ACh effect, suggesting that mAChRs are responsible for the Ca^{2+} increases in the supporting cells (Hegg et al. 2009). We further provide evidence that ACh-induced Ca^{2+} increases are dose dependent. The ACh sensitivity in supporting cells is similar to taste-receptor cells (Ogura 2002), as well as acinar cells of the nasal gland (Fukuda et al. 2008; Gawin et al. 1991; Ikeda et al. 1995). Also, similar to these cells, the

ACh-induced responses consisted of both transient and slow decaying components, and the transient component was largely mediated by Ca^{2+} release from intracellular Ca^{2+} stores. Presently, information regarding the intracellular signaling pathways, which are activated via these mAChRs in supporting cells, remains to be determined. However, several studies have implied that these cells play an important role in regulating extracellular ion and water balance, metabolizing xenobiotic substances, and maintaining olfactory sensitivity and the integrity of the epithelium (Carr et al. 2001; Ding and Dahl 2003; Getchell and Mellert 1991; Hegg et al. 2009; Menco and Morrison 2003). In glandular acinar cells, secretion is tightly coupled to intracellular Ca^{2+} levels (Foskett and Melvin 1989). Thus regulation of the Ca^{2+} levels in supporting cell by ACh may have profound influence on their physiological functions.

ACh-Mediated Modulation of OSNs

In contrast to the robust ACh induced-increases in Ca^{2+} levels in supporting cells, ACh alone did not induce visible Ca^{2+} increases in OSNs in our present study. The absence of ACh-induced intracellular Ca^{2+} increase is not due to enzymatic isolation because our isolated OSNs showed healthy-looking cell bodies as well as multiple long and fine cilia protruding from the dendritic knobs (Supplemental Video S2 and Fig. 4*A*). Also, almost all the OSNs tested responded to the ACIII activator forskolin repeatedly, and a typical percentage of OSNs responded to an odor mixture. The absence of ACh-induced intracellular Ca^{2+} increases found in our study is consistent with a previous report that the ACh agonist muscarine does not induce responses (Firestein and Shepherd 1992).

Interestingly, however, we found that, when OSNs were activated by forskolin, ACh suppressed the evoked Ca^{2+} increases significantly in some OSNs. This suppressive effect is blocked by atropine. Together, the ACh-mediated suppression and the lack of ACh-induced Ca^{2+} increases indicate that the vast majority of OSNs dominantly express an inhibitory subtype of mAChRs and that excitatory mAChRs in the OSNs are relatively weak or absent. Results of our immunolabeling support these notions. We found that the inhibitory subtype M_4 is strongly expressed in the OSNs. We also found that two major stimulatory subtypes M_1 and M_3 are largely absent in the OSNs although they are strongly expressed in supporting cells. Our observed

M_3 immunoexpression is contradictory with a recent finding showing M_3 expression in cilia of the OSNs (Li and Matsunami 2011). Differences in immunolabeling methods, as well as some nonspecific immunoreaction by the Sigma anti-M_3 antibody, likely contribute to the difference between these data. In our study, we used two different antibodies against the M_3 receptor. Both antibodies strongly labeled the supporting cells, and this immunoreactivity was abolished in the M_3 receptor knockout. The Sigma antibody also labeled some OSNs in the ventral region of the MOE with strong reaction in the dendritic knobs. However, this OSN labeling remained in the M_3 receptor knockout with intensity comparable to the OSN labeling in wild-type animals. Thus the labeling in OSNs, especially in the dendritic knob, is nonspecific. We did not observe immunoreaction in the OSN cilia with these two antibodies. In Li and Matsunami's paper (2011), they also reported expression of M_3 mRNA using in situ hybridization. Because we did not examine mRNA expression, we cannot rule out weak expression of M_3 receptor in OSNs, which were not labeled by the antibodies under present conditions. The combination of the weak expression of the stimulatory M_3 and strong expression of inhibitory M_4 may result in the suppressing effect of ACh and lack of ACh-induced Ca^{2+}increase in the OSNs. Li and Matsunami (2011) demonstrated that the mAChR M_3 interacts with odor receptors and that the ACh receptor agonist carbachol potentiates odorant-induced responses in a heterologous expression system. They did not report whether ACh or carbachol increases Ca^{2+} levels in OSNs. In our study we did not detect increases in Ca^{2+} levels in response to ACh in OSNs.

Physiological Function of the Microvillous Cells of the MOE

Our data provide the first physiological evidence showing that ChAT/TRPM5-expressing microvillous cells can be activated by chemical and thermal stimulation. The chemosensitivity of these cells is likely broadly tuned and nonspecific, as we found that these cells react with increases in intracellular Ca^{2+} levels to a variety of chemical stimuli. Presently we do not know the chemical identity in the bacteria lysate responsible for inducing Ca^{2+} responses in the microvillous cells. It will be interesting to determine whether the ATP in the bacterial lysate is a key chemical component to induce these responses. Similar to taste-receptor cells (Kossel et al. 1997; Roper 1983), the ChAT/TRPM5-expressing microvillous cells exhibit

both voltage-gated Na^+ and K^+ currents in electrophysiological studies, indicating that these cells are excitable (Lin et al. 2008a). The notion that these microvillous cells are chemosensitive is supported by the fact that they reside superficially in the MOE with their microvilli extending into the mucus layer, allowing direct contact with inhaled chemicals.

The ChAT/TRPM5-expressing microvillous cells are not the only population of microvillous cells in the mammalian MOE that are chemosensitive. Previously, Elsaesser et al. (2005) reported that a population of microvillous cells is responsive to odor stimulation. These cells are TRPM5 negative but express the transient receptor potential channel C6 and other elements of a phosphatidyl-inositide signaling pathway. A recent study from Hegg et al. (2010) further indicates that these are nonneuronal microvillous cells and that they can respond to odorants and ATP (Hegg et al. 2010). The chemoresponsiveness of microvillous cells may explain our previous findings obtained from cyclic nucleotide-gated channel A2 subunit knockout (CNGA2) mice (Lin et al. 2004). In these knockout mice, the canonical cAMP signaling pathway is paralyzed, rendering the MOE largely insensitive to common volatile odorants. However, many odorants tested at concentrations of 0.5 mM and above induced small changes in the electroolfactogram (EOG). These EOG responses to common odorants generally do not associate with olfactory bulb activation, ruling out the contribution of the noncanonical pathway in OSNs of CNGA2 knockout mice (Lin et al. 2004). The functional consequence of the ACh-mediated suppressive effect in OSNs is not known. It is possible that the microvillous cells react to higher levels of odorants and release ACh to prevent OSNs from being overly activated. The protective function may also be indirect in the intact epithelium in which ACh released from TRPM5/ChAT microvillous cells first activates supporting cells, and the activity of supporting cells modulates OSNs.

We found that the most significant functional implication in the TRPM5/ChAT-expressing microvillous cells is their ability to synthesize and potentially release ACh. These cells are apically located and evenly distributed in the MOE and septal organ. Most likely they constitute the major source of the ACh release intrinsic in the MOE. Recently, when commenting on the modulation of olfactory receptor signaling by M_3 type of mAChR activity (Li and Matsunami 2011), Hall (2011) considered that ACh

is released from parasympathetic nerve endings innervating the olfactory epithelium. However, cholinergic nerves fibers are found mainly in the vascular walls and glandular structures (Chen et al. 1993; Clerico et al. 2003; Grote et al. 1975; Zielinski et al. 1989) within the lamina propria. Consistent with these early studies, we found ChAT-expressing cholinergic nerve fibers, which either are ChAT immunoreactive in TRPM5-GFP mice or GFP positive in ChAT$^{(BAC)}$-eGFP transgenic mice, mainly in the respiratory epithelium, vascular walls, and submucosal glands (data not shown). Given that the M_3 mAChR reported by Li and Matsunami (2011) is localized at the cilia of OSNs, ACh molecules released from autonomic nerves in the lamina propria are unlikely to travel to the cilia of OSNs and to exert the modulatory effects. Therefore, we consider it is likely that ACh is released from the TRPM5/ChAT-expressing microvillous cells.

In summary, we provide evidence showing that the TRPM5-expressing microvillous cells are cholinergic, representing a novel source of ACh synthesis that is intrinsic in the MOE. We also show that ACh modulates activities of supporting cells and OSNs and that the responses are correlated to the differential expression of mAChR subtypes. We further show that the TRPM5/ChAT-expressing microvillous cells are sensitive to chemical stimulation and cold. Thus the TRPM5/ChAT microvillous cells likely play multiple important roles and contribute to the olfactory activity of the MOE.

GRANTS

This work was supported by NIH/NIDCD 009269 and ARRA administrative supplement to W. Lin.

DISCLOSURES

No conflicts of interest, financial or otherwise, are declared by the authors.

Supplementary Material

Supplemental Videos:

Click here to view.

ACKNOWLEDGMENTS

We thank Drs. R. F. Margolskee, M. I. Kotlikoff, and J. Wess for providing us original mouse breeder pairs; Wangmei Luo, Ramon Cabrera, and Ejiofor Ezekwe for technical assistance; and David Dunston and Sarah Ashby for critical readings.

Article information

J Neurophysiol. 2011 Sep; 106(3): 1274–1287.

Published online 2011 Jun 15. doi: 10.1152/jn.00186.2011

PMCID: PMC3174807

PMID: 21676931

Tatsuya Ogura, Steven A. Szebenyi, Kurt Krosnowski, Aaron Sathyanesan, Jacqueline Jackson, and Weihong Lin

Department of Biological Sciences, University of Maryland, Baltimore County, Baltimore, Maryland

REFERENCES

- Bezencon C, Furholz A, Raymond F, Mansourian R, Metairon S, Le Coutre J, Damak S. Murine intestinal cells expressing Trpm5 are mostly brush cells and express markers of neuronal and inflammatory cells. J Comp Neurol 509: 514–525, 2008 [PubMed] [Google Scholar]
- Brockhoff A, Behrens M, Massarotti A, Appendino G, Meyerhof W. Broad tuning of the human bitter taste receptor hTAS2R46 to various sesquiterpene lactones, clerodane and labdane diterpenoids, strychnine, and denatonium. J Agric Food Chem 55: 6236–6243, 2007 [PubMed] [Google Scholar]
- Bryant B, Silver WL. Chemisthesis: The common chemical sense. New York: Wiley-Liss, 2000, pp. 73–100 [Google Scholar]
- Carr VM, Menco BP, Yankova MP, Morimoto RI, Farbman AI. Odorants as cell-type specific activators of a heat shock response in the rat olfactory mucosa. J Comp Neurol 432: 425–439, 2001 [PubMed] [Google Scholar]

- Caulfield MP, Birdsall NJ. International Union of Pharmacology. XVII. Classification of muscarinic acetylcholine receptors. Pharmacol Rev 50: 279–290, 1998 [PubMed] [Google Scholar]
- Chen Y, Getchell TV, Sparks DL, Getchell ML. Patterns of adrenergic and peptidergic innervation in human olfactory mucosa: age-related trends. J Comp Neurol 334: 104–116, 1993 [PubMed] [Google Scholar]
- Clapp TR, Medler KF, Damak S, Margolskee RF, Kinnamon SC. Mouse taste cells with G protein-coupled taste receptors lack voltage-gated calcium channels and SNAP-25 (Abstract). BMC Biol 4: 7, 2006 [PMC free article] [PubMed] [Google Scholar]
- Clerico DA, To WC, Lanza DC. Anatomy of the human nasal passages. In: Handbook of Olfaction and Gestation, 2nd ed, edited by Doty RL. New York: Marcel Dekker, 2003, pp. 1–16 [Google Scholar]
- Dasso LL, Buckler KJ, Vaughan-Jones RD. Muscarinic and nicotinic receptors raise intracellular Ca^{2+} levels in rat carotid body type I cells. J Physiol 498: 327–338, 1997 [PMC free article][PubMed] [Google Scholar]
- Deshpande DA, Wang WC, McIlmoyle EL, Robinett KS, Schillinger RM, An SS, Sham JS, Liggett SB. Bitter taste receptors on airway smooth muscle bronchodilate by localized calcium signaling and reverse obstruction. Nat Med 16: 1299–1304, 2010 [PMC free article] [PubMed] [Google Scholar]
- Ding X, Dahl AR. Olfactory mucosa: composition, enzymatic localization, metabolism. In: Handbook of Olfaction and Gustation, 2nd ed, edited by Doty RL. New York: Marcel Dekker, 2003, pp. 51–73 [Google Scholar]
- Elsaesser R, Montani G, Tirindelli R, Paysan J. Phosphatidyl-inositide signalling proteins in a novel class of sensory cells in the mammalian olfactory epithelium. Eur J Neurosci 10: 2692–700, 2005 [PubMed] [Google Scholar]
- Elsaesser R, Paysan J. The sense of smell, its signalling pathways, and the dichotomy of cilia and microvilli in olfactory sensory cells (Abstract). BMC Neurosci 8, Suppl 3: S1, 2007 [PMC free article] [PubMed] [Google Scholar]
- Farbman A. Cell biology of olfactory epithelium. In: The Neurobiology of Taste and Smell, edited by Finger TE, Silver WL, Restrepo D. New York: Wiley-Liss, 2000, pp. 131–158 [Google Scholar]
- Felder CC. Muscarinic acetylcholine receptors: signal transduction through multiple effectors. FASEB J 9: 619–625, 1995 [PubMed] [Google Scholar]

- Finger TE, St Jeor VL, Kinnamon JC, Silver WL. Ultrastructure of substance P- and CGRP-immunoreactive nerve fibers in the nasal epithelium of rodents. J Comp Neurol 294: 293–305, 1990 [PubMed] [Google Scholar]
- Finger TE, Bottger B, Hansen A, Anderson KT, Alimohammadi H, Silver WL. Solitary chemoreceptor cells in the nasal cavity serve as sentinels of respiration. Proc Natl Acad Sci USA 100: 8981–8986, 2003 [PMC free article] [PubMed] [Google Scholar]
- Firestein S, Shepherd GM. Neurotransmitter antagonists block some odor responses in olfactory receptor neurons. Neuroreport 3: 661–664, 1992 [PubMed] [Google Scholar]
- Foskett JK, Melvin JE. Activation of salivary secretion: coupling of cell volume and $[Ca^{2+}]_i$ in single cells. Science 244: 1582–1585, 1989 [PubMed] [Google Scholar]
- Fukuda N, Shirasu M, Sato K, Ebisui E, Touhara K, Mikoshiba K. Decreased olfactory mucus secretion and nasal abnormality in mice lacking type 2 and type 3 IP3 receptors. Eur J Neurosci27: 2665–2675, 2008 [PubMed] [Google Scholar]
- Gawin AZ, Emery BE, Baraniuk JN, Kaliner MA. Nasal glandular secretory response to cholinergic stimulation in humans and guinea pigs. J Appl Physiol 71: 2460–2468, 1991 [PubMed] [Google Scholar]
- Getchell ML, Mellert TK. Olfactory mucus secretion. In: Smell and Taste in Health and Disease, edited by Getchell TV, Doty RL, Bartoshuk L, Snow JB. New York: Raven Press, 1991, pp. 83–95 [Google Scholar]
- Gross EA, Swenberg JA, Fields S, Popp JA. Comparative morphometry of the nasal cavity in rats and mice. J Anat 135: 83–88, 1982 [PMC free article] [PubMed] [Google Scholar]
- Grote JJ, Juijpers W, Huygen PL. Selective denervation of the autonomic nerve supply of the nasal mucosa. Acta Otolaryngol (Stockh) 79: 124–132, 1975 [PubMed] [Google Scholar]
- Gulbransen BD, Clapp TR, Finger TE, Kinnamon SC. Nasal solitary chemoreceptor cell responses to bitter and trigeminal stimulants in vitro. J Neurophysiol 99: 2929–2937, 2008 [PMC free article] [PubMed] [Google Scholar]
- Hall RA. Autonomic modulation of olfactory signaling. Sci Signal 4: , 2011 [PubMed] [Google Scholar]
- Hansen A, Finger TE. Is TrpM5 a reliable marker for chemosensory cells? Multiple types of microvillous cells in the main olfactory epithelium of

mice (Abstract). BMC Neurosci 9: 115, 2008 [PMC free article] [PubMed] [Google Scholar]
- Hedlund B, Shepherd GM. Biochemical studies on muscarinic receptors in the salamander olfactory epithelium. FEBS Lett 162: 428–431, 1983 [PubMed] [Google Scholar]
- Hegg CC, Irwin M, Lucero MT. Calcium store-mediated signaling in sustentacular cells of the mouse olfactory epithelium. Glia 57: 634–644, 2009 [PMC free article] [PubMed] [Google Scholar]
- Hegg CC, Jia C, Chick WS, Restrepo D, Hansen A. Microvillous cells expressing IP3 receptor type 3 in the olfactory epithelium of mice. Eur J Neurosci 32: 1632–1645, 2010 [PMC free article] [PubMed] [Google Scholar]
- Ikeda K, Ishigaki M, Wu D, Sunose H, Suzuki M, Ishitani K, Takasaka T. Intracellular Ca^{2+} responses induced by acetylcholine in the submucosal nasal gland acinar cells in guinea pigs. Am J Physiol Lung Cell Mol Physiol 268: L361–L367, 1995 [PubMed] [Google Scholar]
- Kaske S, Krasteva G, Konig P, Kummer W, Hofmann T, Gudermann T, Chubanov V. TRPM5, a taste-signaling transient receptor potential ion-channel, is a ubiquitous signaling component in chemosensory cells (Abstract). BMC Neurosci 8: 49, 2007 [PMC free article] [PubMed] [Google Scholar]
- Kossel AH, McPheeters M, Lin W, Kinnamon SC. Development of membrane properties in taste cells of fungiform papillae: functional evidence for early presence of amiloride-sensitive sodium channels. J Neurosci 17: 9634–9641, 1997 [PMC free article] [PubMed] [Google Scholar]
- Kummer W, Lips KS, Pfeil U. The epithelial cholinergic system of the airways. Histochem Cell Biol 130: 219–234, 2008 [PMC free article] [PubMed] [Google Scholar]
- Li YR, Matsunami H. Activation state of the m3 muscarinic acetylcholine receptor modulates mammalian odorant receptor signaling. Sci Signal 4: , 2011 [PMC free article] [PubMed] [Google Scholar]
- Lin W, Arellano J, Slotnick B, Restrepo D. Odors detected by mice deficient in cyclic nucleotide-gated channel subunit A2 stimulate the main olfactory system. J Neurosci 24: 3703–3710, 2004 [PMC free article] [PubMed] [Google Scholar]

- Lin W, Margolskee R, Donnert G, Hell SW, Restrepo D. Olfactory neurons expressing transient receptor potential channel M5 (TRPM5) are involved in sensing semiochemicals. Proc Natl Acad Sci USA 104: 2471–2476, 2007 [PMC free article] [PubMed] [Google Scholar]
- Lin W, Ezekwe EA, Jr, Zhao Z, Liman ER, Restrepo D. TRPM5-expressing microvillous cells in the main olfactory epithelium. BMC Neurosci 9: 114, 2008a [PMC free article] [PubMed] [Google Scholar]
- Lin W, Ogura T, Margolskee RF, Finger TE, Restrepo D. TRPM5-expressing solitary chemosensory cells respond to odorous irritants. J Neurophysiol 99: 1451–1460, 2008b [PubMed] [Google Scholar]
- Menco BP, Morrison EE. Morphology of the mammalian olfactory epithelium: Form, fine structure, function, and pathology. In: Handbook of Olfaction and Gustation, 2nd ed, edited by Doty RL. New York: Marcel Dekker, 2003, pp. 17–50 [Google Scholar]
- Menini A, Pifferi S. New whiffs about chemesthesis. Focus on "TRPM5-expressing solitary chemosensory cells respond to odorous irritants". J Neurophysiol 99: 1055–1056, 2008 [PubMed] [Google Scholar]
- Ogura T. Acetylcholine increases intracellular Ca^{2+} in taste cells via activation of muscarinic receptors. J Neurophysiol 87: 2643–2649, 2002 [PubMed] [Google Scholar]
- Ogura T, Lin W. Acetylcholine and acetylcholine receptors in taste receptor cells. Chem Senses 30, Suppl 1: i41, 2005 [PubMed] [Google Scholar]
- Ogura T, Mackay-Sim A, Kinnamon SC. Bitter taste transduction of denatonium in the mudpuppy Necturus maculosus. J Neurosci 17: 3580–3587, 1997 [PMC free article] [PubMed] [Google Scholar]
- Ogura T, Margolskee RF, Kinnamon SC. Taste receptor cell responses to the bitter stimulus denatonium involve Ca^{2+} influx via store-operated channels. J Neurophysiol 87: 3152–3155, 2002 [PubMed] [Google Scholar]
- Ogura T, Krosnowski K, Zhang L, Bekkerman M, Lin W. Chemoreception regulates chemical access to mouse vomeronasal organ: role of solitary chemosensory cells. PLos One 5: e11924, 2010 [PMC free article] [PubMed] [Google Scholar]
- Ogura T, Margolskee RF, Tallini YN, Shui B, Kotlikoff MI, Lin W. Immuno-localization of vesicular acetylcholine transporter in mouse taste cells

and adjacent nerve fibers: indication of acetylcholine release. Cell Tissue Res 330: 17–28, 2007 [PubMed] [Google Scholar]
- Papka RE, Matulionis DH. Association of substance-P-immunoreactive nerves with the murine olfactory mucosa. Cell Tissue Res 230: 517–525, 1983 [PubMed] [Google Scholar]
- Resende RR, Adhikari A. Cholinergic receptor pathways involved in apoptosis, cell proliferation and neuronal differentiation (Abstract). Cell Commun Signal 7: 20, 2009 [PMC free article][PubMed] [Google Scholar]
- Rome C, Luo D, Dulon D. Muscarinic receptor-mediated calcium signaling in spiral ganglion neurons of the mammalian cochlea. Brain Res 846: 196–203, 1999 [PubMed] [Google Scholar]
- Roper S. Regenerative impulses in taste cells. Science 220: 1311–1312, 1983 [PubMed] [Google Scholar]
- Sekerkova G, Zheng L, Loomis PA, Changyaleket B, Whitlon DS, Mugnaini E, Bartles JR. Espins are multifunctional actin cytoskeletal regulatory proteins in the microvilli of chemosensory and mechanosensory cells. J Neurosci 24: 5445–5456, 2004 [PMC free article] [PubMed] [Google Scholar]
- Shah AS, Ben-Shahar Y, Moninger TO, Kline JN, Welsh MJ. Motile cilia of human airway epithelia are chemosensory. Science 325: 1131–1134, 2009 [PMC free article] [PubMed] [Google Scholar]
- Shigemoto T, Ohmori H. Muscarinic agonists and ATP increase the intracellular Ca^{2+} concentration in chick cochlear hair cells. J Physiol 420: 127–148, 1990 [PMC free article] [PubMed] [Google Scholar]
- Sokal RR, Rohlf FJ. The comparison of dendrograms by objective methods. Taxonomy 11: 33–40, 1962 [Google Scholar]
- Stannard W, O'Callaghan C. Ciliary function and the role of cilia in clearance. J Aerosol Med 19: 110–115, 2006 [PubMed] [Google Scholar]
- Tallini YN, Shui B, Greene KS, Deng KY, Doran R, Fisher PJ, Zipfel W, Kotlikoff MI. BAC transgenic mice express enhanced green fluorescent protein in central and peripheral cholinergic neurons. Physiol Genomics 27: 391–397, 2006 [PubMed] [Google Scholar]
- Tizzano M, Cristofoletti M, Sbarbati A, Finger TE. Expression of taste receptors in Solitary Chemosensory Cells of rodent airways. BMC Pulm Med 11: 3, 2011 [PMC free article] [PubMed] [Google Scholar]
- Tizzano M, Gulbransen BD, Vandenbeuch A, Clapp TR, Herman JP, Sibhatu HM, Churchill ME, Silver WL, Kinnamon SC, Finger TE. Nasal

chemosensory cells use bitter taste signaling to detect irritants and bacterial signals. Proc Natl Acad Sci USA 107: 3210–3215, 2010 [PMC free article] [PubMed] [Google Scholar]
- Trotier D. Electrophysiological properties of frog olfactory supporting cells. Chem Senses 3: 363–9, 1998 [PubMed] [Google Scholar]
- Vogalis F, Hegg CC, Lucero MT. Ionic conductances in sustentacular cells of the mouse olfactory epithelium. J Physiol 562: 785–99, 2005a [PMC free article] [PubMed] [Google Scholar]
- Vogalis F, Hegg CC, Lucero MT. Electrical coupling in sustentacular cells of the mouse olfactory epithelium. J Neurophysiol 94: 1001–1012, 2005b [PubMed] [Google Scholar]
- Ward JH. Hierarchical grouping to optimize an objective function. J Am Stat Assoc 48: 236–244, 1963 [Google Scholar]
- Wessler I, Kirkpatrick CJ. Acetylcholine beyond neurons: the non-neuronal cholinergic system in humans. Br J Pharmacol 154: 1558–1571, 2008 [PMC free article] [PubMed] [Google Scholar]
- Yamada M, Miyakawa T, Duttaroy A, Yamanaka A, Moriguchi T, Makita R, Ogawa M, Chou CJ, Xia B, Crawley JN, Felder CC, Deng CX, Wess J. Mice lacking the M3 muscarinic acetylcholine receptor are hypophagic and lean. Nature 410: 207–212, 2001 [PubMed] [Google Scholar]
- Zhang Z, Zhao Z, Margolskee R, Liman E. The transduction channel TRPM5 is gated by intracellular calcium in taste cells. J Neurosci 27: 5777–5786, 2007 [PMC free article] [PubMed] [Google Scholar]
- Zielinski BS, Getchell ML, Wenokur RL, Getchell TV. Ultrastructural localization and identification of adrenergic and cholinergic nerve terminals in the olfactory mucosa. Anat Rec 225: 232–245, 1989 [PubMed] [Google Scholar]